scientific reports

Check for updates

OPEN

Explainable prediction model for punching shear strength of FRP-RC slabs based on kernel density estimation and XGBoost

Sheng Zheng[1], Tianyu Hu[2], Nima Khodadadi[3]✉ & Antonio Nanni[3]

Reinforced concrete (RC) slabs are widely used in modern building structures due to their superior properties and ease of construction. However, their mechanical properties are limited by their punching shear strength in the connection region with the columns. Researchers have attempted to add steel reinforcement in the form of studs and randomly distributed fibers to concrete slabs to improve the punching strength. An additional strengthening method that consists of the application is a Fiber-Reinforced Polymer (FRP). However, current codes poorly calculate the punching shear strength of FRP-RC slabs. The aim of this study is to create a robust model that can accurately predict its punching shear strength, thus improving the analysis and design of composite structures with FRP-RC slabs. In this study, 189 sets of experimental data were collected and expanded using kernel density estimation (KDE), considering the small amount of data. Secondly, a punching shear strength prediction model for FRP-RC panels was constructed using XGBoost and compared with the model modeled by codes and researchers. Finally, a model explainability study was conducted using SHapley additive exPlanations (SHAP). The results show that kernel density estimation significantly improves the robustness and accuracy of XGBoost. The R-squared, standard deviation, and root mean square error of XGBoost on the training set are 0.99, 0.001, and 0.001, respectively. On the test set, the R-squared, standard deviation, and root mean square error are 0.96, 62.687, and 67.484, respectively. The effective depth of the FRP-RC slabs is the most important and proportional to the punching shear strength. This study can provide guidance for the design of FRP-RC slabs.

Keywords Fiber-reinforced polymer, RC slabs, Kernel density estimation, XGBoost, SHapley additive exPlanations

Currently, the use of RC (RC) in conjunction with composite structures has gained extensive popularity. Among them, RC slabs, as a key component in modern building structures, not only carry the load of the building but also reflect the perfect integration of material science and structural engineering[1,2]. In the composite material system of RC, high-strength steel and durable concrete interact with each other to jointly resist external forces and ensure the safety and stability of the structure[3–5]. RC slabs are widely used in the fields of flooring, roofing, and even special structures such as staircases and bridge slabs due to their unique mechanical properties and ease of construction[6–9].

Numerous techniques, such as enclosed loops, bent steel reinforcements, and shear connectors, have been extensively implemented to boost the punching shear resistance of RC slabs. Recently, there has been a surge in scholarly attention towards employing FRP as a reinforcing medium in concrete slabs, intending to augment their capacity to resist punching shear forces. This innovative approach addresses some of the limitations associated with traditional steel reinforcement. The use of FRP in concrete slabs is seen as a significant advancement in construction materials technology, offering improved durability and performance in structural applications[10,11]. Researchers have conducted numerous studies and experiments to understand the behavior and benefits of FRP-RC slabs under various loading conditions, leading to a better understanding of effectively incorporating FRP into concrete structures to optimize their strength and longevity[12–16]. Compared with traditional concrete

[1]Shanghai Urban Construction Vocational College, Shanghai 201415, China. [2]State Key Laboratory of Mountain Bridge and Tunnel Engineering, Chongqing Jiaotong University, Chongqing 400074, China. [3]Department of Civil and Architectural Engineering, University of Miami, Coral Gables, FL 33146, USA. ✉email: nima.khodadadi@miami.edu

slabs, they have the advantages of being lightweight, having good corrosion resistance, high strength, insulation, and fatigue resistance. They are suitable for building structures that require special requirements such as high load-bearing capacity, corrosion resistance, or electrical insulation and have a wider application prospect[17,18].

Various models have been put forth by both codes and researchers to estimate the punching shear strength of concrete slabs reinforced with FRP. Canadian Standards Association (CSA), Japan Society of Civil Engineers (JSCE), and American Concrete Institute (ACI) have proposed punching shear strength prediction models considering the effect of loading area dimensions, effective depth, and concrete strength[19–21]. Besides, Deifalla[17] has proposed a punching shear strength prediction model based on the critical shear crack theory. These models have contributed significantly to the study of this combined structure. However, FRP-RC slabs have a complex structure, and their punching shear strength is subject to the coupling of multiple parameters, which is difficult to achieve by the existing mathematical models and the applicability of the above models still needs to be strengthened as the coefficients of variation of the models are large compared with the experimental values. In addition, Badra et al.[18] constructed a predictive model for the punching strength of FRP-RC slabs using ANN and SVM. Although the accuracy of this model is better than that of the codes' and Deifalla's model, its coefficient of variation is large (0.25 for ANN and 0.2 for SVM), which makes it difficult to guarantee the reliability of the application and lacks explainability. Based on this, a predictive model for punching shear strength of FRP-RC slabs with higher accuracy and explainability is required to be proposed.

In recent years, ensemble learning has been increasingly used in structural engineering due to its much better performance than single learning and its explainability[22,23].

For instance, Khodadadi et al.[24] introduced a pioneering machine-learning approach for predicting the compressive strength of Carbon fiber-reinforced polymer Confined-Concrete (CFRP-CC) specimens. Utilizing a Particle Swarm Optimization-Categorical Boosting (PSO-CatBoost) algorithm, their model, based on an extensive database of 916 experimental outcomes from 105 scholarly articles, demonstrated superior predictive performance compared to six contemporary machine learning models and six empirical models. Their approach uniquely incorporated SHapley Additive exPlanations (SHAP) and Permutation Feature Importance (PFI) methodologies to elucidate feature importance, establishing a new benchmark in CFRP-CC predictive modeling. Taffese et al.[25] collected 170 sets of data, used CatBoost to predict the ultimate moment of UHPC-strengthened beams, and conducted a feature importance study based on SHAP. Sapkota et al.[26] collected 226 data sets, used five ensemble learning models to predict the effective stiffness of rectangular RC columns, and used SHAP to study the sensitivity between input and output parameters. Pal et al.[27] predicted a slump of FRP-RC containing waste rubber and recycled aggregates based on 464 data sets using 12 models, including single and ensemble learning. The results show that XGBoost performs best among all the models. Alyami et al.[28] predicted the compressive strength of concrete containing rice husk based on 348 data sets using three ensemble models and one single model. They carried out an interpretable study of the model using SHAP. The results showed that the ensemble model outperformed the single model, and SHAP explained the key indicators affecting the compressive strength.

This research delves into the application of artificial intelligence algorithms in forecasting the punching shear strength of concrete slabs reinforced with FRP materials. Advanced machine learning techniques are employed, building upon previous research, with a particular emphasis on model interpretability. Methodologies such as SHAP and importance and sensitivity analyses are utilized to clarify the machine learning (ML) results. The most extensive collection of experimental data to date is aggregated, incorporating the highest number of variables into the model-building process compared to previous studies. This comprehensive approach is intended to enhance the understanding of the factors influencing punching shear strength. Specifically, a database of 189 sets of valid data from 36 research papers, including key input variables: loading area shape, loading area dimensions, effective depth, concrete strength, FRP Young's modulus, FRP reinforcement ratio, and output punching shear strength, is compiled. Since the amount of data is crucial to model performance in ML, this study first uses kernel density estimation (KDE) to expand the experimental data. Subsequently, it develops an explainable predictive model for the punching shear strength of FRP-strengthened concrete slabs, grounded on the integration of the XGBoost algorithm with SHAP analysis. The developed ML model is compared against existing formulas. Ultimately, the study identifies the paramount variables influencing punching shear capacity and formulates enhanced predictive equations with improved accuracy.

The follow-up study consists of the following sections: Section "Methodology" introduces the data enhancement model - kernel density estimation - and the integrated learning model - XGBoost - used in this study. Section "Database construction" is the database construction, including experimental data collection and KDE-based data augmentation. Section "Model construction and evaluation" is the model construction and evaluation, including selecting hyperparameters for XGBoost, validating data enhancement effects, evaluating existing codes' and researchers' models, and the explainability study of XGBoost. The last section is the conclusion, which includes a summary of the results obtained in this study and an outlook for future research.

Methodology

Kernel density estimation

Kernel density estimation (KDE) is a non-parametric probability density estimation method determined by the data distribution[29]. For the problem that the distribution of the observed data is unknown, without making any distributional assumptions about it, the probability density function is modeled based on the observed data itself. The formula for KDE is shown in Eq. (1):

$$f_h(y) = \frac{1}{nh}\sum_{i=1}^{n} K\left(\frac{y - y_i}{h}\right), y \in R, \tag{1}$$

where, n is the number of the sample points, denotes the kernel function, denotes the bandwidth, which affects how smooth the probability density estimate is.

Extreme gradient boosting

Extreme Gradient Boosting (XGBoost)[30] is a general-purpose Gradient Boosting algorithm that is capable of carrying out multi-threaded parallel computation with high resistance to overfitting and accuracy (See Fig. 1). XGBoost makes predictions by iteratively building a series of decision trees. The predictions from each tree are combined to form the final prediction. The prediction formula of XGBoost can be expressed as:

$$\begin{aligned} \bar{y}(x) &= \sum_{t=1}^{T} f_t(x) \\ f_t(x) &= w_{q(x)} \end{aligned} \tag{2}$$

Where $\overline{y}(x)$ is the sum of the predicted values of all the decision trees, f_t denotes the predicted value of each decision tree, $w_{q(x)}$ is the function that maps the sample x to the index of the leaf node of the tree.

The objective function of XGBoost mainly consists of loss function and regularisation term, as shown below:

$$\begin{aligned} Obj(\theta) &= \sum_{i=1}^{n} l(y_i, \overline{y_i}) + \sum_{j=1}^{t} \Omega(f_j) \\ \sum_{j=1}^{t} \Omega(f_j) &= \gamma T + \frac{1}{2}\lambda \sum\nolimits_{j=1}^{T} w_j^2 \end{aligned} \tag{3}$$

where T is the number of leaves, w_j is the value associated with the jth leaf, γ is a parameter that penalizes the number of leaves, and λ is the L2 regularization term on the leaf weights. The regularization term of XGBoost penalizes the complexity of the model through the parameters γ and λ to prevent overfitting, thus maintaining the model's generalization ability. For additional information on XGBoost, see reference[30].

Shapley additive explanation

Shapley Additive Explanations (SHAP), rooted in the principles of cooperative game theory, stands out as a prominent model-agnostic technique designed to improve the interpretability of ML models. It quantifies the significance of features through the application of Shapley values, thereby offering a robust framework for understanding model predictions. The SHAP value for a feature is calculated as follows:

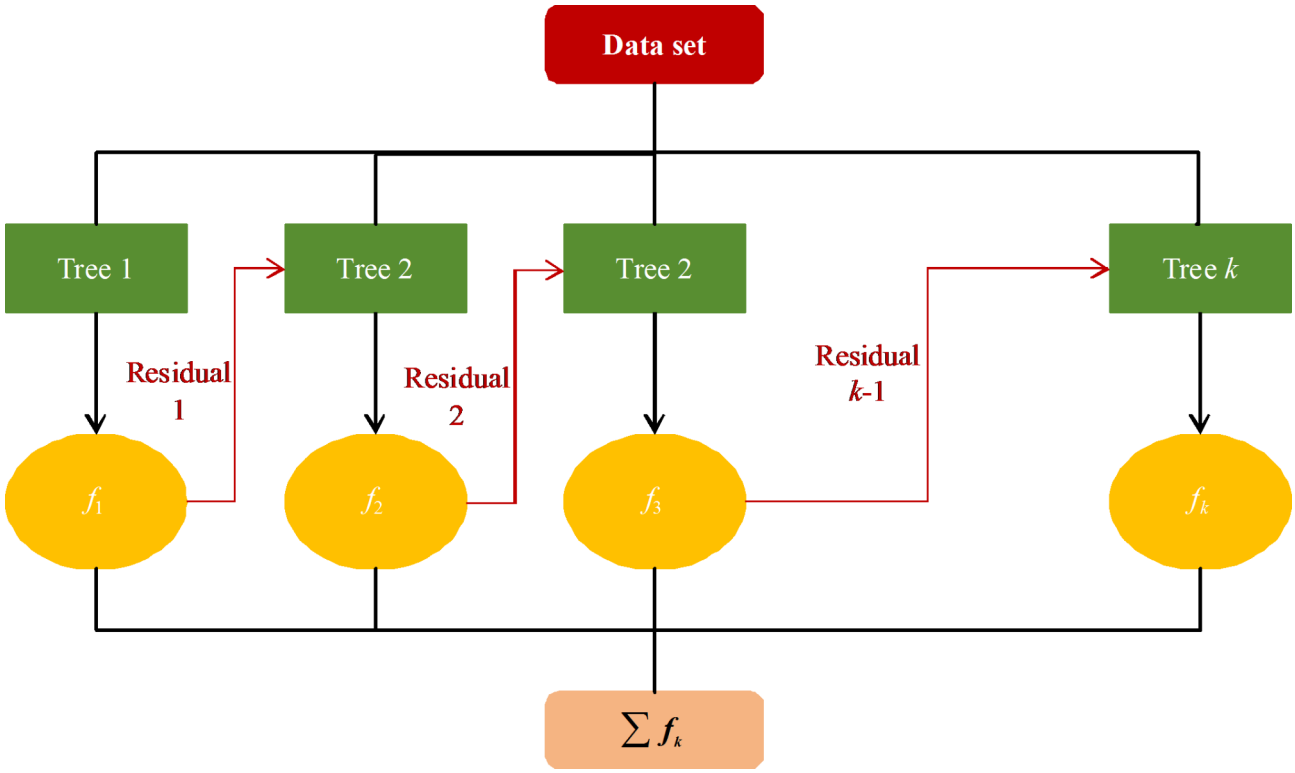

Fig. 1. Architecture of XGBoost.

$$\phi_j(\mathrm{val}) = \sum_{S \subseteq \{1,\ldots,P\} \setminus \{j\}} \frac{|S|!(P-|S|-1)!}{P!} \left(\mathrm{val}(S \cup \{j\}) - \mathrm{val}(S)\right) \tag{4}$$

where S is a feature subset, x is the feature vector, and p is the number of features.

Modelling

The data from Section "Database construction" was used to construct the model based on two methods. These two methods are denoted as N1 and N2, respectively. N1: The dataset was partitioned such that 80% of the experimental instances served as the training subset, while the remaining 20% constituted the testing subset. N2: In an alternative approach, the synthesized data was utilized for training purposes, with the actual experimental data reserved exclusively for testing, thereby validating the model's predictive capabilities. The modeling uses XGBoost, as mentioned in Section "Extreme gradient boosting", and its optimal hyperparameters are obtained using grid search and five-fold cross-validation. Grid search is a method to find the best model hyperparameters by traversing different parameter combinations. Five-fold cross-validation is a commonly used method for model evaluation, and its principle is shown in Fig. 2. Step 1 divides the training dataset into five equal parts; Step 2 uses four parts to train the model and the remaining one to validate the model; Step 2 is repeated until each part is used as a training and validation set; finally, the performance of the model is calculated as the average of the results of the five evaluations.

Database construction

Data details

An aggregation of 189 experimental datasets was compiled from a thorough examination of 36 distinct research endeavors[11–16,31–60], including key input variables: loading area shape (A, B), loading area dimensions (b, c), effective depth (d), cubic concrete strength (f'_c), FRP young modulus (E), FRP reinforcement ratio (ρ), and output: punching shear strength (V). The statistical analysis of the data is shown in Table 1. The distribution of the data is shown in Fig. 3.

As can be seen in Fig. 3, the distribution of the features is wide but uneven across the intervals.

Data expansion

As described in Section "Data details", 189 sets of experimental data were collected. Considering the impact of smaller data sizes on the model generalization performance, this section expands the data based on the kernel density estimation algorithm mentioned in Section "Kernel density estimation". The expanded data contains 689 data sets (500 generated data and 189 experimental data). The distribution of the data before and after the expansion is shown in Fig. 4.

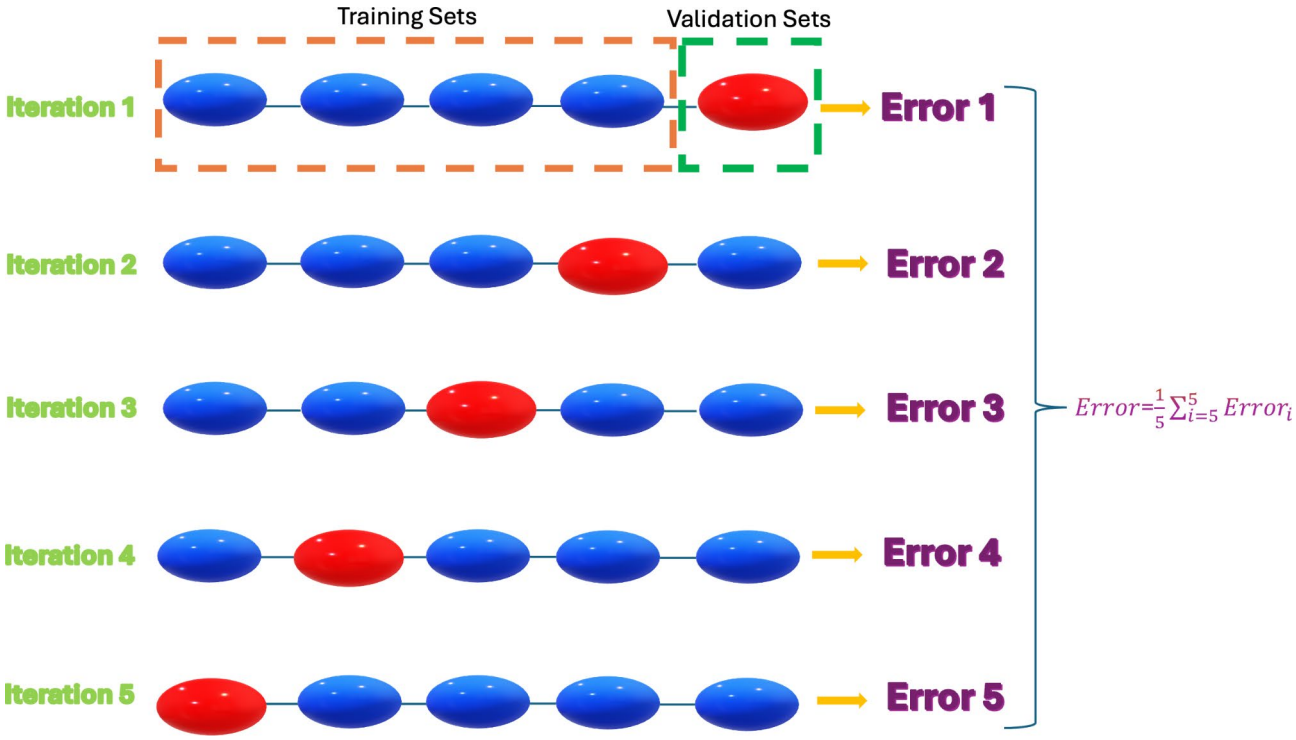

Fig. 2. 5-fold cross-validation.

	A	B	b	c	d	f'_c	ρ	E
Unit	mm	mm	mm	mm	mm	MPa	%	GPa
skew	-0.43	-0.28	0.69	-0.97	0.94	3.43	1.74	1.31
max	3000	4000	635	300	284	179	3.76	230
min	300	300	25	25	45	22.2	0.18	28.4
mean	1960.90	1735.77	300.95	212.20	131.43	45.78	0.94	79.91

Table 1. Statistical characterization of features.

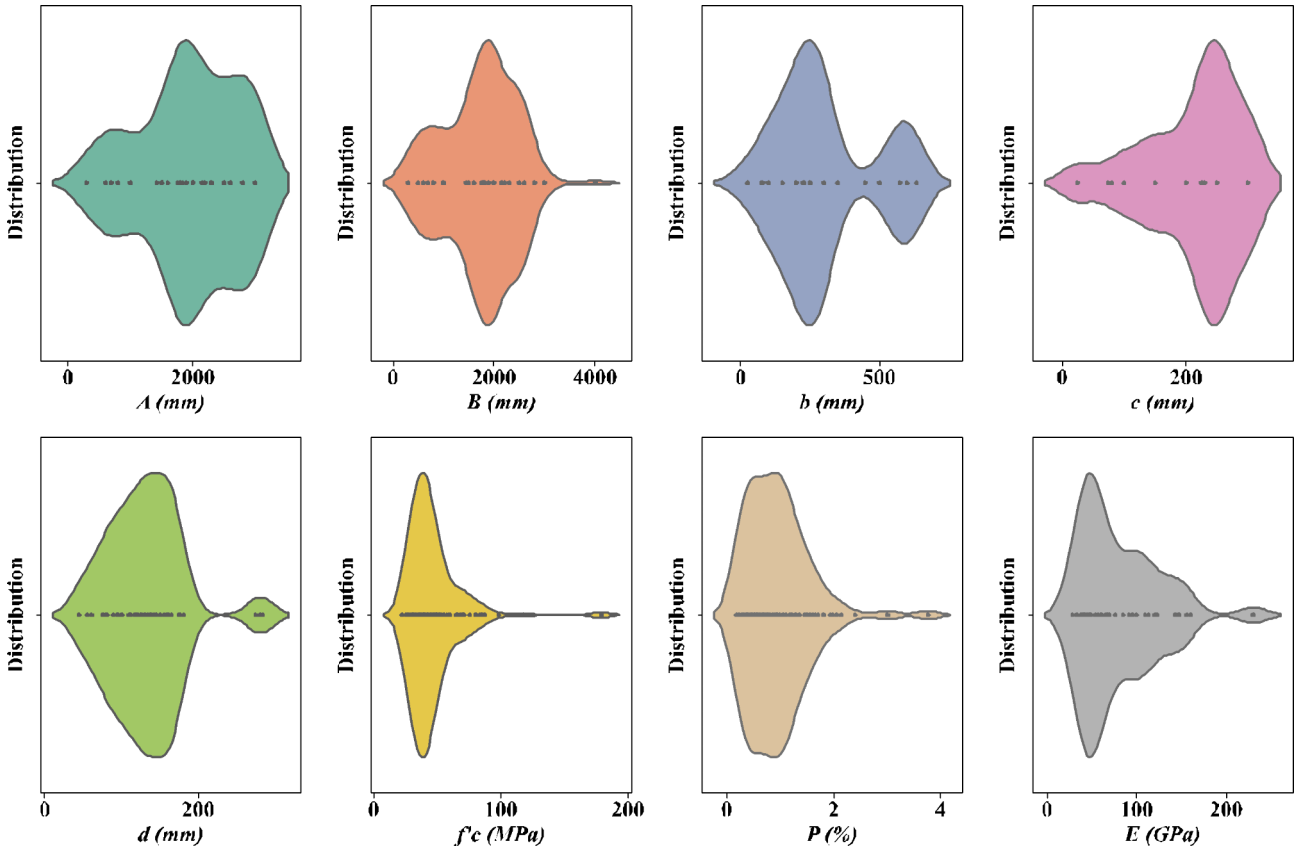

Fig. 3. Distribution of parameters.

In Fig. 4, the first five are geometric features, and the last four are material features. The kernel density function is the same for the enhanced data and the original data, which indicates that the kernel density estimation model learns the feature distribution of the original data well.

Model construction and evaluation

Data enhancement validation

A comparison of training and test set prediction results and experimental values of XGBoost model before and after data enhancement is shown in Fig. 5.

As can be seen from Fig. 5, the XGBoost model outperforms N1 on the training set under N2, but the difference on the test set is not significant. To further validate the effectiveness of data enhancement, the distribution of deviations on the training and test sets of the model under N1 and N2 are given in Fig. 6.

As can be seen in Fig. 6, the model has better robustness (normal deviation distribution) under both N1 and N2. However, it is evident that the deviation distributions of the model training and test sets under N2 are closer to 0, indicating that it is more robust than N1. Figures 5 and 6. confirm the robustness of the data-augmented model, and further, the table gives the R-squared (R^2), standard deviation (SD), and root-mean-square error (RMSE) of the model training and test sets before and after augmentation.

As can be seen from Table 2, the data-augmented model has a smaller improvement in R^2 on the training set, but there is a significant reduction in SD and RMSE. In addition, the performance of the data-enhanced model in terms of R^2, SD, and RMSE on the test set substantially improved. To further highlight the superiority of XGBoost, it is compared with Logistic Regression (LR), Backpropagation (BP), Support Vector Machine (SVM),

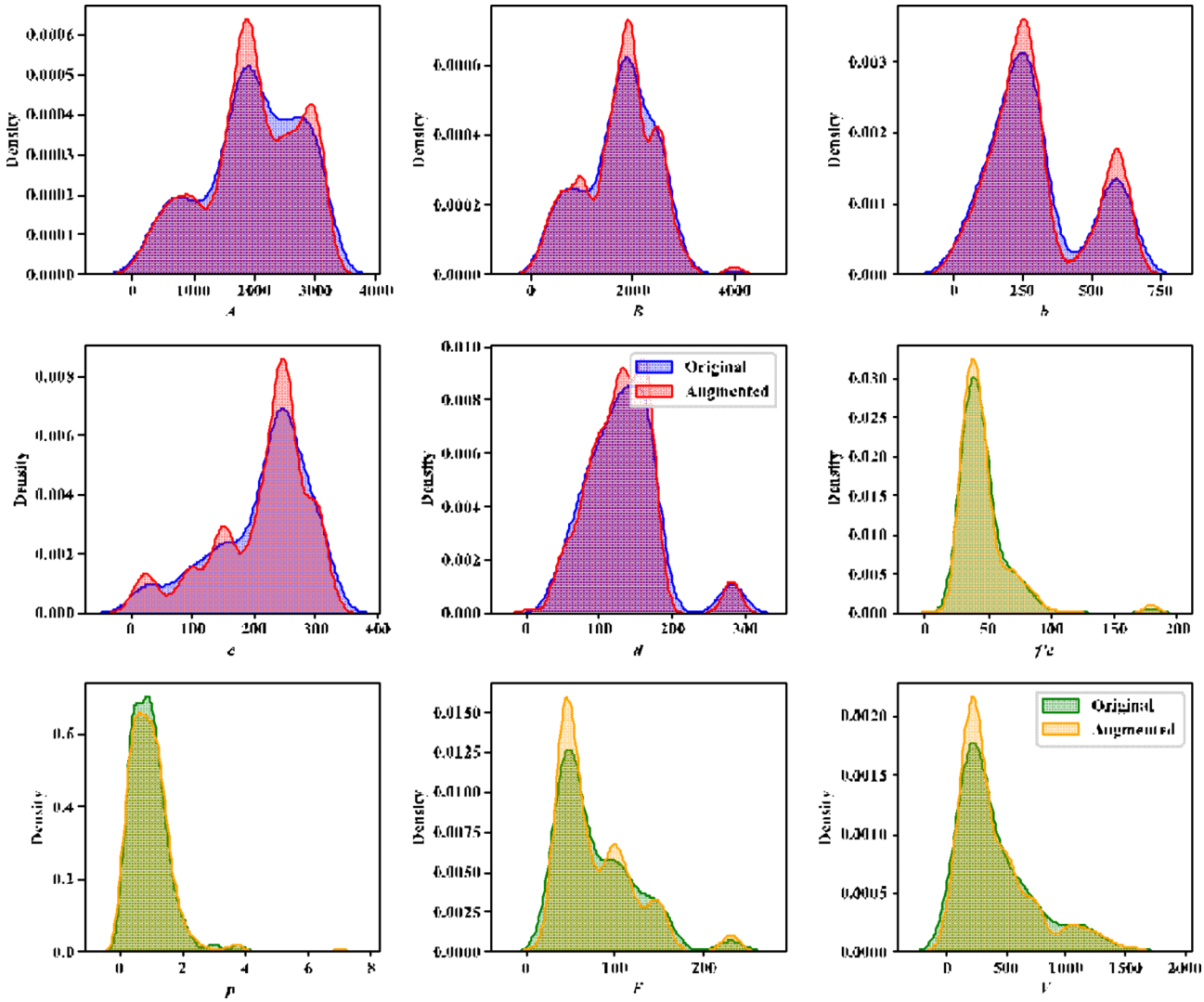

Fig. 4. Distribution of features before and after data augmentation.

Decision Tree (DT), and Random Forest (RF) under N2. The hyperparameters of the ML model are shown in Table 3, and the RMSE and R^2 are shown in Table 4. As can be seen from Table 3, the performance of XGBoost is significantly better than that of the other models.

Model evaluation

The existing models for calculating the punching shear strength of FRP-RC slabs are shown in Table 5.

Figure 7 illustrates the comparative performance of the model developed within this research against existing models.

Figure 7 shows that the models suggested by codes and researchers have low R-squared and coefficients of variation of more than 60%, which makes them unsuitable for guiding engineering practice. The XGBoost model constructed in this study has very high R-squared and coefficients of variation within 20%, which is much better than existing models.

Model explainability

From Sections "Model evaluation" and "Model explainability", it can be seen that XGBoost performs better with data augmentation, and therefore, an explainable study of the model is performed using XGBoost under N2. The explainability of the model is performed through SHAP. SHAP is an ML model explanation tool based on Shapley values, which helps to understand and explain the decision-making process of complex models by decomposing model predictions into the contribution of individual features, providing both local and global explanations[26,28]. The global explainability of XGBoost is shown in Figs. 8 and 9, and the local explainability is shown in Fig. 10 using the SHAP force plot. It is important to note that in these figures, yellow indicates a positive impact, and green indicates a negative impact.

Figure 8 analyses the importance of the parameters in terms of the entire data set. As can be seen in Fig. 8, overall, d and B have the most significant impact on punching shear strength, while ρ and E have a lesser impact

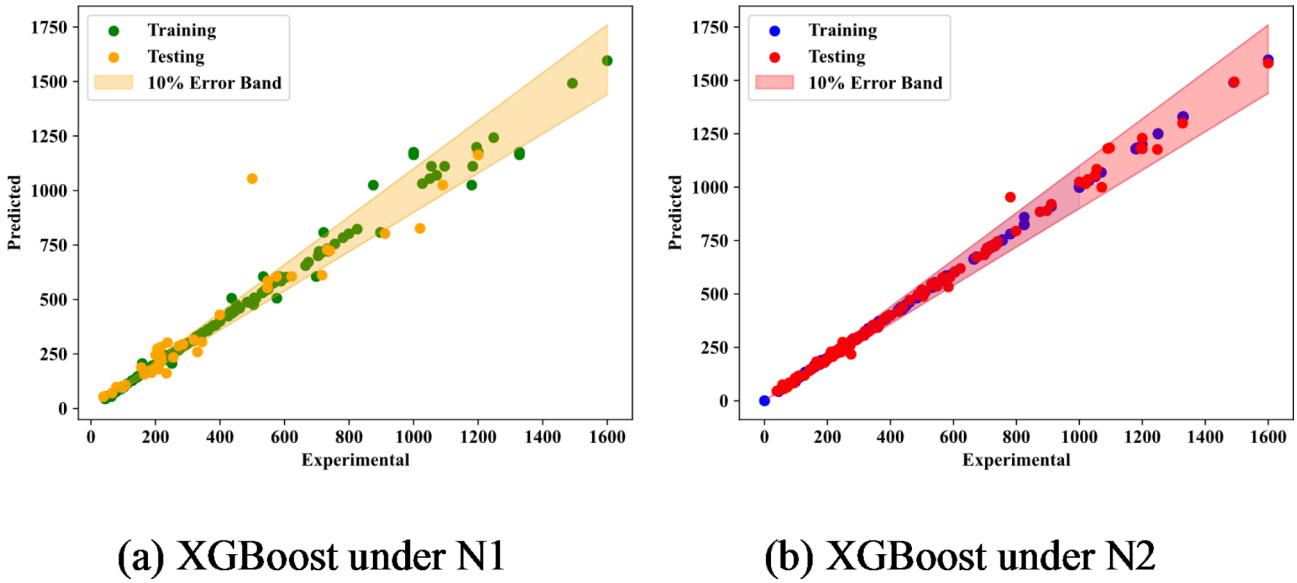

Fig. 5. Model predictions vs. real values under N1 and N2.

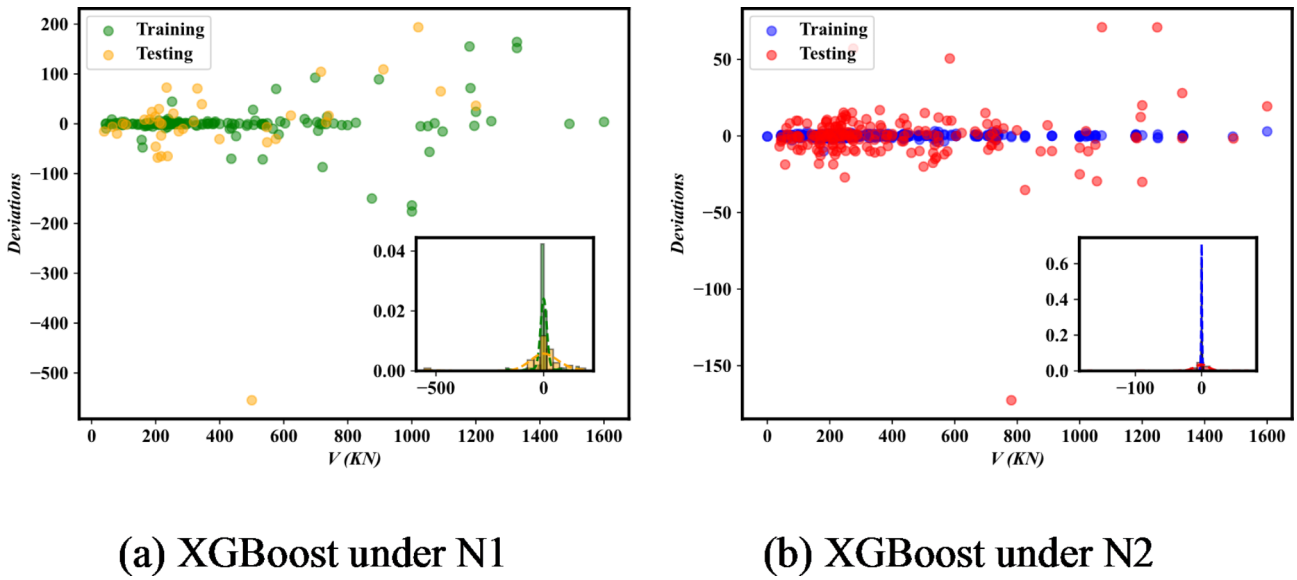

Fig. 6. Distribution of deviations under A and B.

	N1-Training	N2-Training	N1-Test	N2-Test
R^2	0.987	0.999	0.878	0.976
SD	37.336	0.806	103.661	20.309
RMSE (kN)	37.336	0.806	103.777	20.312

Table 2. Performance of the model under N1 and N2.

on punching shear strength. On the other hand, Fig. 9 provides a sensitivity analysis of the parameters from the perspective of the entire dataset. Taking the first four parameters with higher importance as an example, it can be seen from Fig. 9 that all the four parameters with higher importance have a positive effect on the punching shear strength, i.e., the punching shear strength will be improved as d, B, A, and b increases.

Figures 8 and 9 analyze the importance and sensitivity of the parameters from a global point of view. However, the parameters' importance and sensitivity tend to differ for different samples. Figure 10 gives the predicted

	hyperparameters
LR	-
SVM	kernel='linear', C = 0.3 (0.001,1000), epsilon = 0.1 (0.001,1)
BP	hidden_layer_sizes = 14 (2,20), activation='relu', solver='adam'
DT	max_depth = 15 (2,100), min_samples_split = 2 (2,10), min_samples_leaf = 2 (2,10)
RF	n_estimators = 513 (10,1000), max_depth = 18 (2,100), min_samples_split = 8 (2,10), min_samples_leaf = 3 (2,10)
XGB	max_depth = 2 (2,100), learning_rate = 0.6 (0.01,1), n_estimators = 100 (10,1000), alpha = 4.7 (1,10), lambda = 4.9 (1,10)

Table 3. Hyperparameters of the ML models.

	Training		Testing	
	RMSE (kN)	R^2	RMSE (kN)	R^2
LR	142.41	0.82	142.71	0.80
SVM	169.19	0.73	172.18	0.71
BP	95.33	0.91	116.57	0.87
DT	24.24	0.99	76.81	0.94
RF	15.65	0.99	71.15	0.95
XGBoost	0.11	0.99	67.18	0.96

Table 4. Performance of different models under N2.

Refs.	Formula	Symbols
(JSCE) [20]	$V = \beta_d \beta_\rho \beta_r f_{Pcd} b_{0.5d} d$	$\beta_d = \left(\frac{1000}{d}\right)^{\frac{1}{4}} \leqslant 1.5\beta_\rho = (100\rho E/E_S)^{\frac{1}{3}} \leqslant 1.5\beta_r$ $= 1 + \frac{1}{\left(1 + \frac{0.25 b_{0.5d}}{d}\right)} f_{Pcd} = 0.2\sqrt{f'_c} \leqslant 1.2 b_{0.5d} = 4(c+d)$
(CSA) [19]	$V = b_{0.5d} d \begin{cases} 0.028(1 + \frac{2}{\beta_c})\left(E\rho f'_c\right)^{\frac{1}{3}} \\ 0.147\left(E\rho f'_c\right)^{\frac{1}{3}}\left(0.19 + \alpha_s \frac{d}{b_{0.5d}}\right) \\ 0.056\left(E\rho f'_c\right)^{\frac{1}{3}} \end{cases}$	$\beta_c = 1, \alpha_s = 4$ $b_{0.5d} = 4(c+d)$
(ACI) [21]	$V = 0.8\sqrt{f'_c} k d b_{0.5d}$	$k = \sqrt{2\rho n + (\rho n)^2} - \rho n n = 4750\sqrt{f'_c} b_{0.5d} = 4(c+d)$
Deifalla [17]	$\psi = 0.28 \frac{r_s}{d} \frac{f_f}{E} \left(\frac{V}{V_{flex}}\right)^{0.4}$	$V_{flex} = 2\pi m_R \frac{r_s}{r_q - r_c}, m_R = d^2 \rho f_f \left(1 - \frac{\rho f_f}{2 f'_c \left(\frac{30}{f'_c}\right)^{\frac{1}{3}}}\right)$

Table 5. Existing models.

overlay for two different samples. The former sample is from Hassan et al.[48], and the latter is from Fareed et al.[52]. In Fig. 10, the arrows and directions indicate the effect of parameters on punching shear strength. Yellow indicates a positive influence, and green indicates a negative influence.

Figure 10 demonstrates that the importance and sensitivity of features to punching shear strength are different in different samples. For example, for the two samples mentioned above, the top four ranked features have exactly the same effect on punching shear strength, but ρ is inversely related to punching shear strength in the first sample and the opposite in the second sample. Similarly, E has a negative effect on punching shear strength in the first sample but a positive effect in the second sample. It is important to note that even though the effects of the features are not exactly the same in both samples, XGBoost predicts them both better. The experimental value of the first sample is 329KN, and the model predicts 338.15KN with an error of 2.7%. The second sample had an experimental value of 548KN, and the model predicted 555.58KN with an error of 1.3%.

GUI

To make the XGBoost models practical for users, a user-friendly graphical user interface (GUI) was developed. This GUI incorporates the key input features identified in the study, enabling users to generate two types of outputs. Figure 11 shows a screenshot of the GUI designed to predict the punching shear strength of FRP-RC slabs, utilizing kernel density estimation and XGBoost. The interface is streamlined and intuitive, making complex predictions easy with just a few clicks—users input the required data and receive the output. Accessible

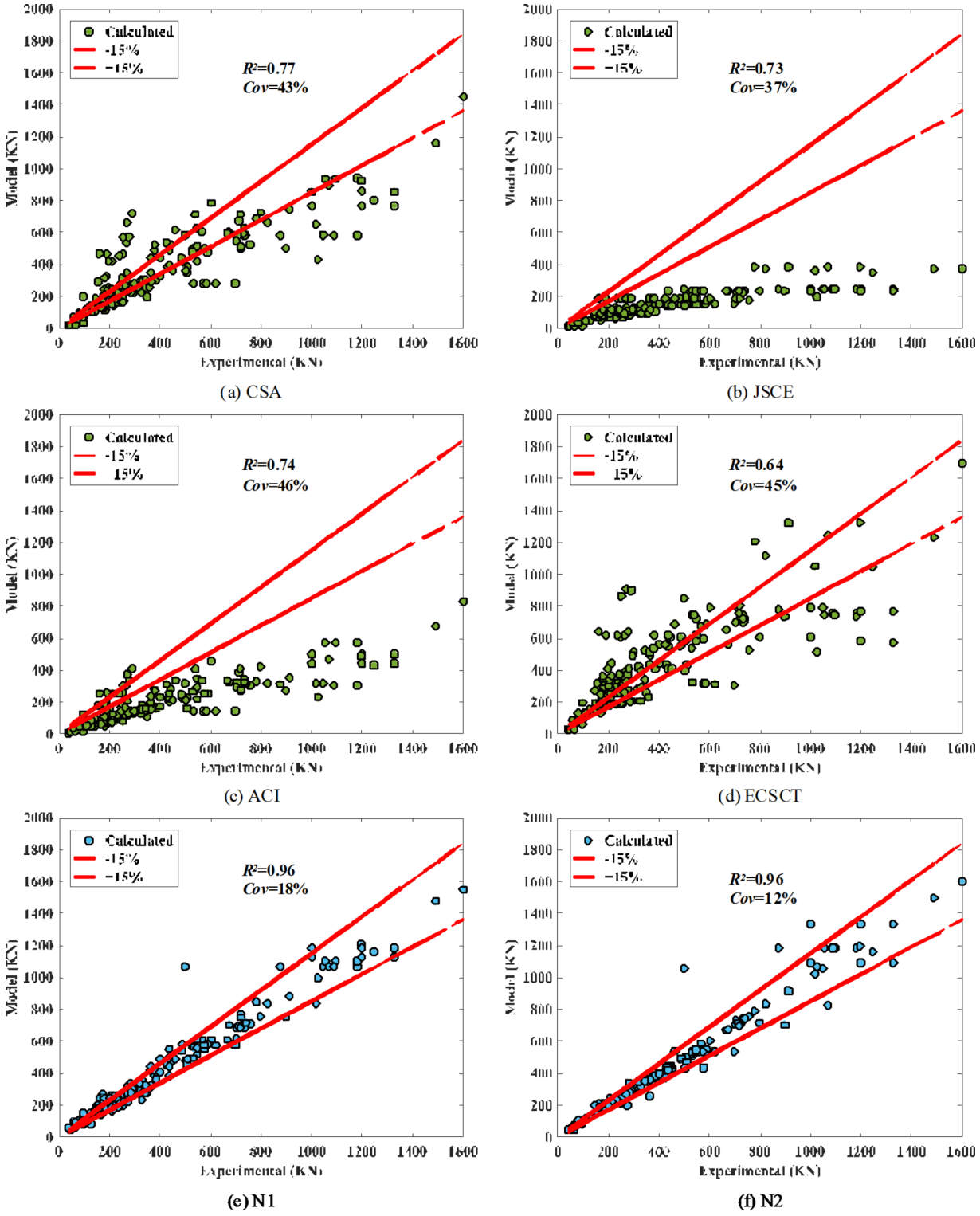

Fig. 7. Model evaluation.

at "https://nimakhodadadi.com/softwares," this tool is particularly useful for educational purposes, offering a hands-on learning experience in material properties without requiring deep technical knowledge. The input ranges displayed alongside each feature guide users to provide realistic values, improving the tool's reliability. In summary, this GUI is a practical, accessible, and educational resource for both professionals and students in construction and materials science.

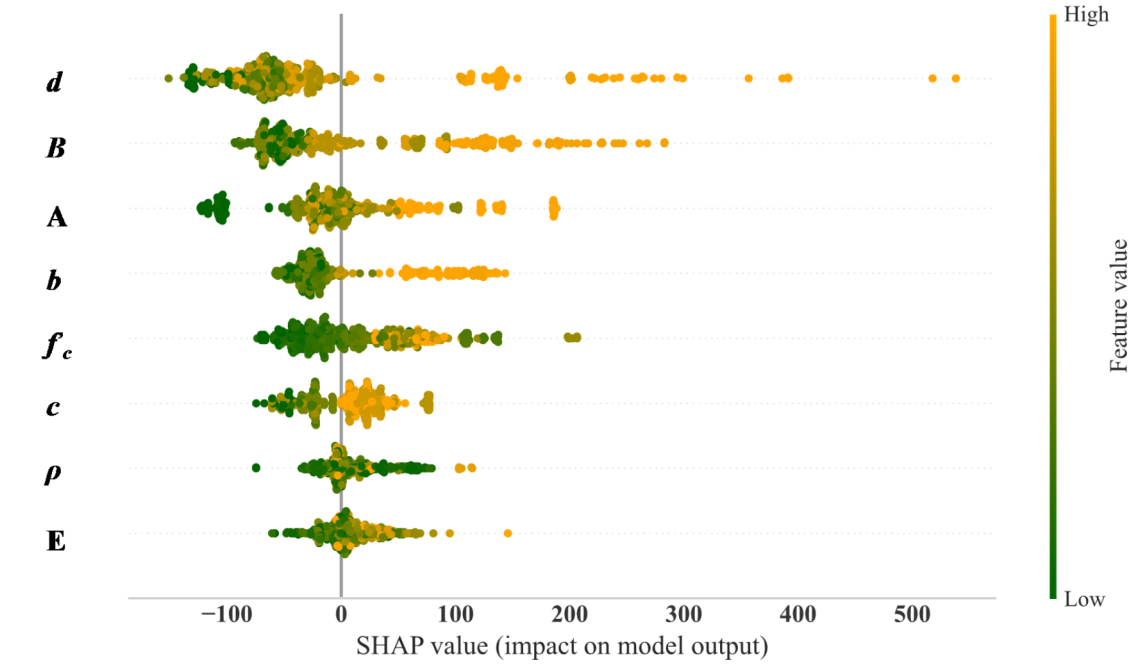

(a) SHAP summary plot

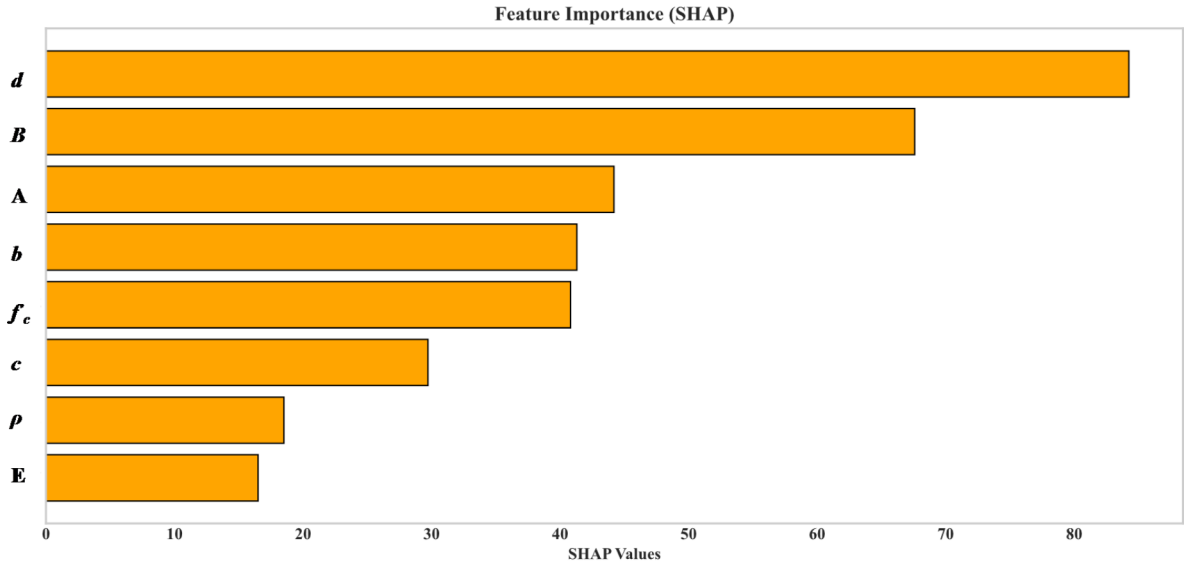

(b) Feature importance plot

Fig. 8. Importance study of parameters.

Conclusion

This study aimed to develop an accurate and robust prediction model for the punching shear strength of FRP-reinforced concrete slabs using the XGBoost ensemble learning model. Kernel Density Estimation (KDE) was used for data augmentation, and model interpretability was enhanced through SHapley Additive exPlanations (SHAP). Additionally, a graphical user interface (GUI) was designed to facilitate engineers' use. The study led to the following conclusions:

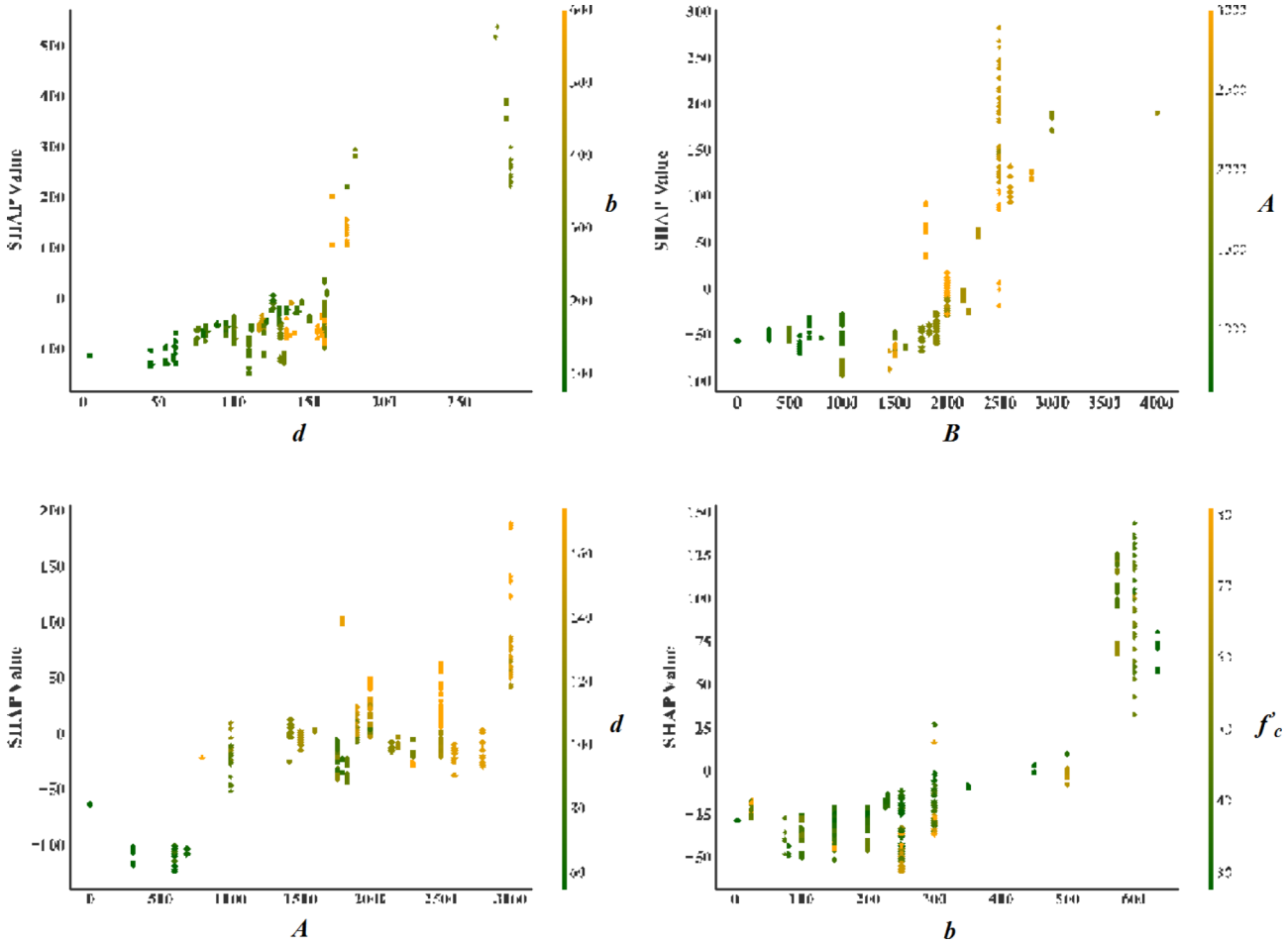

Fig. 9. Sensitivity study of parameters.

- Kernel density estimation can generate feature data for FRP-RC slabs. It significantly enhances the robustness and precision of ML predictive models. The augmented model's R-squared on the training and test sets is higher than before augmentation, and the standard deviation and root mean square error are much lower.
- The existing codes and the models suggested by researchers for calculating the punching shear strength of FRP-RC slabs have low R-squared (below 0.8) and coefficients of variation exceeding 60%, which are not conducive to practical engineering applications.
- Of all the ML models used in this paper, XGBoost performed the best. On the training and test sets, it had the smallest RMSE and the largest R^2.
- The effective depth (d) of the FRP-RC slabs is the most important and proportional to the punching shear strength. ρ and E have a lesser influence on the punching shear strength and have a more complex relationship with the punching shear strength.

This study extends the application of KDE in structural engineering and demonstrates the performance of the XGBoost model in predicting the punching shear strength of FRP-RC slabs. In addition, the conclusions on the significance and sensitivity of the features obtained in this study can be used as a reference for code revision and engineering design of FRP-RC slabs. However, this study is data-driven and does not incorporate knowledge of the mechanics of FRP-RC slabs, and further refinement of the model with professional knowledge is required in the future.

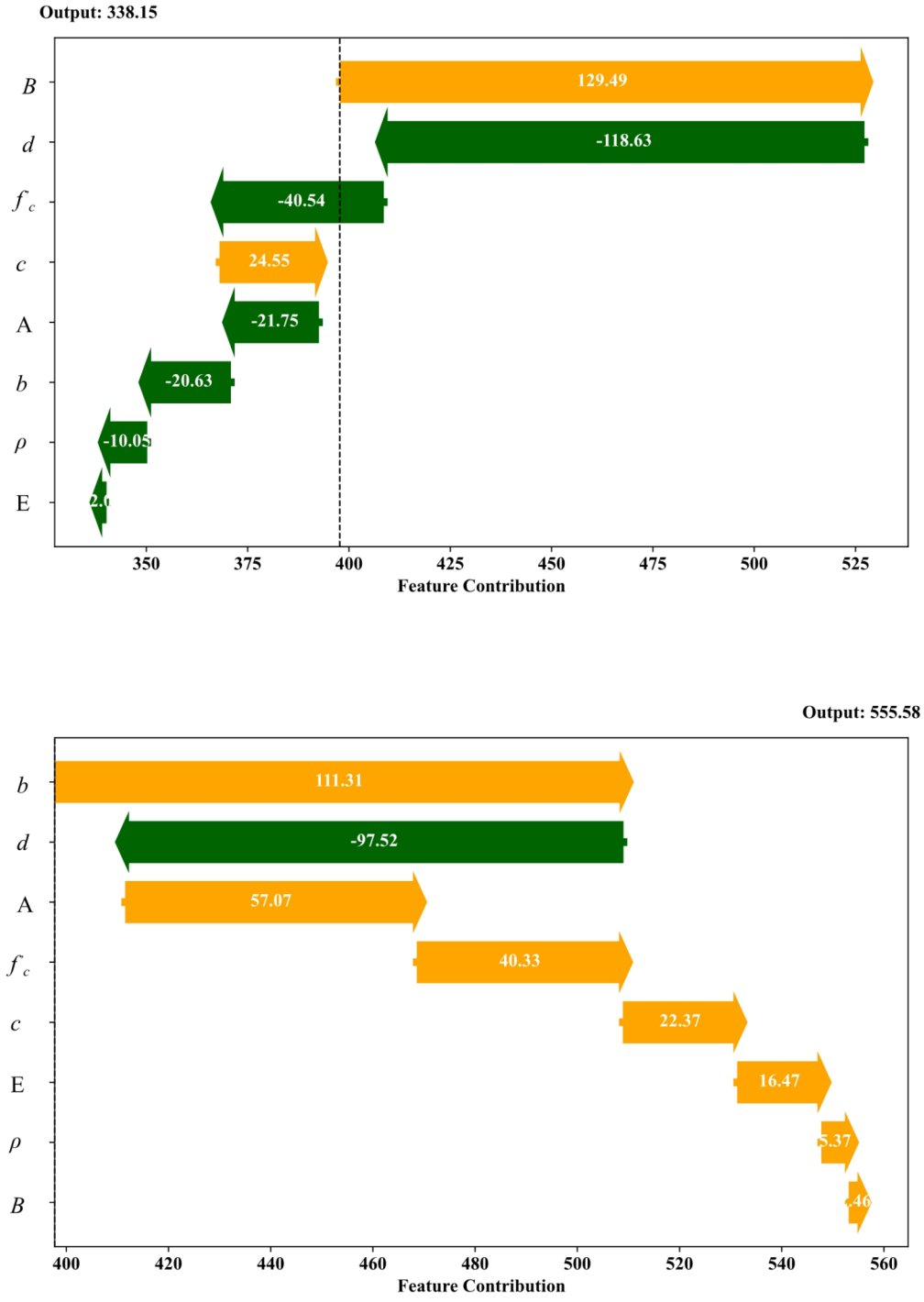

Fig. 10. SHAP waterfall plot.

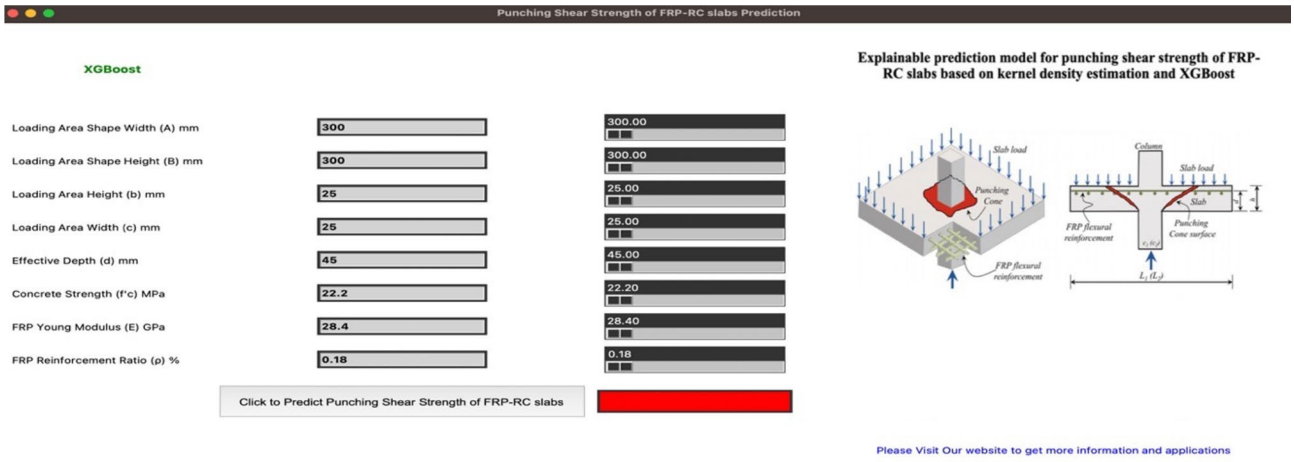

Fig. 11. GUI designed to predict the punching shear strength of FRP-RC slabs (https://nimakhodadadi.com/softwares).

Data availability

The datasets used and/or analyzed during the current study are available from the corresponding author on reasonable request.

Received: 2 July 2024; Accepted: 3 December 2024
Published online: 30 December 2024

References

1. Hafez, H. et al. Decarbonization potential of steel fibre-reinforced limestone calcined clay cement concrete one-way slabs. *Constr. Build. Mater.* **435**, 136847 (2024).
2. Zhao, X. et al. Experimental and mesoscopic modeling numerical researches on steel fiber reinforced concrete slabs under contact explosion. *Structures*(2024).
3. Al-Darzi, S. Y. The effect of using shredded plastic on the behavior of reinforced concrete slab. *Case Stud. Constr. Mater.* **17**, e01681 (2022).
4. Djamai, Z. I. et al. PCM-modified textile-reinforced concrete slab: a multiscale and multiphysics investigation. *Constr. Build. Mater.* **293**, 123483 (2021).
5. Zakaria, D. et al. Two-way shear full behavior of reinforced concrete flat slabs under membrane tensile forces. *Case Stud. Constr. Mater.* **18**, e01912 (2023).
6. Hassanli, R. et al. Investigation of punching shear performance in concrete slabs reinforced with GFRP and synthetic fibers: an experimental study. *Eng. Struct.* **311**, 118215 (2024).
7. Yan, J. et al. Explainable machine learning models for punching shear capacity of FRP Bar reinforced concrete flat slab without shear reinforcement. *Case Stud. Constr. Mater.* **20**, e03162 (2024).
8. Han, T. et al. An investigation of the flexural behaviour of large-span prestressed and steel-reinforced concrete slabs. *Sci. Rep.* **13**(1), 10710 (2023).
9. Ors, D. M. et al. Machine learning base models to predict the punching shear capacity of posttensioned UHPC flat slabs. *Sci. Rep.* **14**(1), 3969 (2024).
10. Wakjira, T. G. et al. FAI: fast, accurate, and intelligent approach and prediction tool for flexural capacity of FRP-RC beams based on super-learner machine learning model. *Mater. Today Commun.* **33**, 104461 (2022).
11. Al-Hamrani, A. et al. Sensitivity analysis and genetic algorithm-based shear capacity model for basalt FRC one-way slabs reinforced with BFRP bars. *Compos. Struct.* **305**, 116473 (2023).
12. Khodadadi, N. et al. Fiber-reinforced polymer (FRP) in concrete: a comprehensive survey. *Constr. Build. Mater.* **432**, 136634 (2024).
13. Banthia, N., Al-Asaly, M. & Ma, S. Behavior of concrete slabs reinforced with fiber-reinforced plastic grid. *J. Mater. Civ. Eng.* **7**(4), 252–257 (1995).
14. Bank, L. C. Punching Shear Behavior of Pultruded FRP Grating Reinforced Concrete Slabs. *Non-Metallic (FRP) Reinforcement for Concrete Structures: Proceedings of the Second International RILEM Symposium* Vol. 29. (CRC Press, 1995).
15. Louka, H. J. *Punching behaviour of a hybrid reinforced concrete bridge deck* MS thesis (1999).
16. Bouguerra, K. et al. Testing of full-scale concrete bridge deck slabs reinforced with fiber-reinforced polymer (FRP) bars. *Constr. Build. Mater.* **25**(10), 3956–3965 (2011).
17. Deifalla, A. Punching shear strength and deformation for FRP-reinforced concrete slabs without shear reinforcements. *Case Stud. Constr. Mater.* **16**, e00925 (2022).
18. Alkhatib, S. & Ahmed, D. Punching shear strength of FRP-reinforced concrete slabs without shear reinforcements: a reliability assessment. *Polymers* **14**(9), 1743 (2022).
19. CSA. *Design and Construction of Building Structures with Fiber Reinforced Polymers (CAN/CSA S806-12)* (2012).
20. JSCE. Recommendation for Design and Construction of Concrete Structures Using Continuous Fiber Reinforcing Materials, Concrete Engineering Series 23, A. Machida, Ed., Tokyo, Japan 325 (1997).
21. ACI-440. Guide for the Design and Construction of Concrete Reinforced with FRP Bars (ACI 440.1R-15)., ACI, Farmington Hills, Michigan, USA (2015).
22. Wakjira, T. G., Abushanab, A. & Alam, M. S. Hybrid machine learning model and predictive equations for compressive stress-strain constitutive modelling of confined ultra-high-performance concrete (UHPC) with normal-strength steel and high-strength steel spirals. *Eng. Struct.* **304**, 117633 (2024).

23. Wakjira, T. G., Kutty, A. A. & Alam, M. S. A novel framework for developing environmentally sustainable and cost-effective ultra-high-performance concrete (UHPC) using advanced machine learning and multi-objective optimization techniques. *Constr. Build. Mater.* **416**, 135114 (2024).
24. Khodadadi, N. et al. Data-driven PSO-CatBoost machine learning model to predict the compressive strength of CFRP-confined circular concrete specimens. *Thin-Walled Struct.* **198**, 111763 (2024).
25. Taffese, W. Z., Zhu, Y. & Chen, G. Ensemble-learning model based ultimate moment prediction of reinforced concrete members strengthened by UHPC. *Eng. Struct.* **305**, 117705 (2024).
26. Sapkota, S. C., Das, S. & Saha, P. Optimized machine learning models for prediction of effective stiffness of rectangular reinforced concrete column sections. *Structures* Vol. 62 (Elsevier, 2024).
27. Pal, A., Ahmed, K. S. & Mangalathu, S. Data-driven machine learning approaches for predicting slump of fiber-reinforced concrete containing waste rubber and recycled aggregate. *Constr. Build. Mater.* **417**, 135369 (2024).
28. Alyami, M. et al. Estimating compressive strength of concrete containing rice husk ash using interpretable machine learning-based models. *Case Stud. Constr. Mater.* **20**, e02901 (2024).
29. Węglarczyk, S. Kernel density estimation and its application. ITM web of conferences. Vol. 23 (EDP Sciences, 2018).
30. Wakjira, T. G. & Alam, M. A. Performance-based seismic design of Ultra-high-performance concrete (UHPC) bridge columns with design example-powered by explainable machine learning model. *Eng. Struct.* **314**, 118346 (2024).
31. Rahman, A. H., Kingsley, C. Y. & Kobayashi, K. Service and ultimate load behavior of bridge deck reinforced with carbon FRP grid. *J. Compos. Constr.* **4**(1), 16–23 (2000).
32. Hassan, T. et al. Fibre reinforced Polymer reinforcing bars for bridge decks. *Can. J. Civ. Eng.* **27**(5), 839–849 (2000).
33. Zaghloul, A. *Punching Shear Strength of Interior and edge column-slab Connections in CFRP Reinforced flat Plate Structures Transferring Shear and Moment* (Diss. Carleton University, 2007).
34. El-Ghandour, A. W., Pilakoutas, K. & Waldron, P. Punching shear behavior of fiber reinforced polymers reinforced concrete flat slabs: Experimental study. *J. Compos. Constr.* **7**(3), 258–265 (2003).
35. El-Ghandour, A. W., Pilakoutas, K. & Waldron, P. Punching shear behavior of fiber reinforced polymers reinforced concrete flat slabs: Experimental study. *J. Compos. Constr.* **7**(3), 258–265 (2003)
36. Ospina, C. E. et al. Punching of two-way concrete slabs with fiber-reinforced polymer reinforcing bars or grids. *Struct. J.* **100**(5), 589–598 (2013).
37. Hussein, A., Rashid, I. & Benmokrane, B. Two-way concrete slabs reinforced with GFRP bars. *Proceedings of the 4th International Conference on Advanced Composite Materials in Bridges and Structures, Calgary, Alberta* (2004).
38. Jacobson, D. A. et al. Punching shear capacity of double layer FRP grid reinforced slabs. *Proc., 7th International Conference on Fiber Reinforced Plastics for Reinforced Concrete Structures* (2005).
39. El-Gamal, S., El-Salakawy, E. & Benmokrane, B. Behavior of concrete bridge deck slabs reinforced with fiber-reinforced polymer bars under concentrated loads. *ACI Struct. J.* **102**(5), 727 (2005).
40. Zhang, Q., Marzouk, H. & Hussein, A. A preliminary study of high-strength concrete two-way slabs reinforced with GFRP bars. *Proceedings of the 33rd CSCE Annual Conference: General Conference and International History Symposium* (2005).
41. El-Tom, E. *Behavior of Two-Way Slabs Reinforced with GFRP Bars* (Memorial University of Newfoundland, 2007).
42. Zaghloul, E. E. R., Mahmoud, Z. I. & Salama, T. A. Punching behavior and strength of two-way concrete slabs reinforced with glass fiber reinforced polymer (GFRP) rebars. In *Proceedings of the Structural Composites for Infrastructure Applications, Hurghada, Egypt* 1–16 (2007).
43. El-Gamal, S., El-Salakawy, E. & Benmokrane, B. Influence of reinforcement on the behavior of concrete bridge deck slabs reinforced with FRP bars. *J. Compos. Constr.* **11**(5), 449–458 (2007).
44. Ramzy, Z. & Salma, Z. M. T. Punching behavior and strength of two-way concrete slab reinforced with glass-fiber reinforced polymer (GFRP) rebars. In *Proceedings of the Structural Composites forInfrastructures Applications Conference, Hurghada, Egypt* (2007).
45. Zaghloul, E. E. R., Mahmoud, Z. I. & Salama, T. A. Punching behavior and strength of two-way concrete slabs reinforced withglass fiber reinforced polymer (GFRP) rebars. In *Proceedings of StructuralComposites for Infrastructure Applications, Hurghada, Egypt* 1–16. (2008).
46. Lee, J. H. et al. Improving punching shear behavior of glass fiber-reinforced polymer reinforced slabs. *ACI Struct. J.* **106**(4), 427 (2009).
47. Zhu, H. et al. Deformation behavior of concrete two-way slabs reinforced with BFRP bars subjected to eccentric loading. *Advances in FRP Composites in Civil Engineering: Proceedings of the 5th International Conference on FRP Composites in Civil Engineering (CICE 2010), Sep 27–29, 2010, Beijing, China* (2011).
48. Min, K-H. et al. Flexural and punching performances of FRP and fiber reinforced concrete on impact loading. *Advances in FRP Composites in Civil Engineering: Proceedings of the 5th International Conference on FRP Composites in Civil Engineering (CICE 2010), Sep 27–29, 2010, Bei**g, China* (2011).
49. Xiao, Z. *Experimental Study on two-way Concrete slab Subjected to Punching Shear* (Diss. Zhengzhou University, 2010).
50. Nguyen-Minh, L. & Rovňák, M. Punching shear resistance of Interior GFRP reinforced slab-column connections. *J. Compos. Constr.* **17**(1), 2–13 (2013).
51. Hassan, M., Ahmed, E. & Benmokrane, B. Punching-shear strength of normal and high-strength two-way concrete slabs reinforced with GFRP bars. *J. Compos. Constr.* **17**(6), 04013003 (2013).
52. El-gendy, M. & El-Salakawy, E. Punching shear behaviour of GFRP-RC edge slab-column connections. In *Proceedings of the Seventh International Conference on FRP Composites in Civil Engineering* 1–6 (2015).
53. Tharmarajah, G., Taylor, S. E., Cleland, D. J. & Robinson, D. Corrosion-resistant FRP reinforcement for bridge deck slabs. In *Proceedings of the Institution of Civil Engineers. Bridge Engineering 168 September Issue BE3* 208–217 (2015).
54. Mostafa, A. Punching Shear Behavior of GFRP-RC Slab-Column EdgeConnections with High Strength Concrete and Shear Reinforcement (M.Sc.thesis) (Manitoba university, 2016).
55. Fareed, E., Ahmed, E. A. & Benmokrane, B. Experimental testing of concrete bridge-deck slabs reinforced with Basalt-FRP reinforcing bars under concentrated loads. *J. Bridge Eng.* **21**, 7 (2016).
56. Gouda, A. & El-Salakawy, E. Punching shear strength of GFRP-RC Interior slab–column connections subjected to moment transfer. *J. Compos. Constr.* **04015037**, 0000597 (2016).
57. Oskouei, A. V., Kivi, M. P., Araghi, H. & Bazli, M. Experimental study of the punching behavior of GFRP reinforced lightweight concrete footing. *Mater. Struct.* **50**, 256 (2017).
58. Hussein, A. H. & El-Salakawy, E. F. Punching shear behavior of glass fiber-reinforced polymer-reinforced concrete slab-column interior connections. *Acids Struct. J.* **115**(4) (2020).
59. Hemzah, S. A., Al-Obaidi, S. & Salim, T. Punching shear model for normal and high-strength concrete slabs reinforced with CFRP or steel bars, Jordan *J. Civ. Eng.* **13**(2) (2019).
60. Huang, Z., Zhao, Y., Zhang, J. & Wu, Y. Punching shear behavior of concrete slabs reinforced with CFRP grids. *Structures* **26**(2020), 617–625 (2020).

Acknowledgements
The authors gratefully acknowledge the financial support from the National Science Foundation I/U-CRC Center for Integration of Composites into Infrastructure (CICI) under grant #1916342.

Author contributions
Sh.Zh: Conceptualization, Methodology, Writing – original draft, Visualization. T.H: Conceptualization, Data curation, Writing – original draft, Visualization, Formal analysis. N.Kh: Writing – original draft, Methodology, Visualization, Investigation, Software. A.N: Resources, Writing – review & editing, Supervision.

Declarations

Competing interests
The authors declare no competing interests.

Ethical approval
This article does not contain any studies with human participants or animals performed by any of the authors. Informed consent was not required as no human or animals were involved.

Additional information
Correspondence and requests for materials should be addressed to N.K.

Reprints and permissions information is available at www.nature.com/reprints.

Publisher's note Springer Nature remains neutral with regard to jurisdictional claims in published maps and institutional affiliations.